Reprinted from THE JOURNAL OF CHEMICAL PHYSICS, Vol. 40, No. 2, 415–422, 15 January 1964
Printed in U. S. A.

Origin of OH Chemiluminescence during the Induction Period of the H_2–O_2 Reaction behind Shock Waves

F. E. BELLES AND M. R. LAUVER

NASA. Lewis Research Center, National Aeronautics and Space Administration, Cleveland, Ohio 44135

(Received 16 September 1963)

The intensity and the rate of increase of light emitted by the $OH^* {}^2\Sigma^+ \rightarrow {}^2\Pi$ (0–0) transition were studied during the induction period behind shock waves in 5% H_2–95% air mixture. Induction-zone temperatures ranged from about 1000° to 1900°K, and the initial pressure was 10 Torr. A standard lamp was used to calibrate the optical system, so that photomultiplier signals could be transformed to OH^* concentration. The results are interpreted in terms of radical-recombination reactions. It is found that OH^* is formed in the reaction $H+O_2+H_2 \rightarrow H_2O+OH^*$ and is effectively quenched, in these experiments, only by water. The excitation process is an inefficient reaction, with an average rate constant of 2×10^5 liter^2/mole^2·sec.

INTRODUCTION

THE combustion of H_2 and O_2 is accompanied by the emission of ultraviolet light, due almost entirely to the transition of the excited radical $OH^*({}^2\Sigma^+)$ to the ground state ($^2\Pi$). An understanding of the processes leading to this emission is of interest because it would provide further information on the details of this reaction. Such understanding would also be of value in other ways: It might permit use of the emitted light as an indication of the progress of the main reactions and it would allow quantitative comparisons to be made between induction times measured by following the concentration of ground state OH with absorption spectroscopy[1] and those measured by the easier method of observing the emitted light.[2]

For many years, evidence (summarized in Ref. 3) has accumulated favoring both a thermal and a nonthermal (chemiluminescent) origin of the excited state of OH in the H_2–O_2 reaction. More recently, Kaskan[4] studied the OH^* emission from H_2–O_2–N_2 flame gases, in which the concentrations of the free radicals H, O, and OH are in excess of the equilibrium values. He found that the radiation arises from recombination reactions among these excess free radicals. The intensity of emission was found to be proportional to the third power of the ground-state OH concentration (which was measured by absorption), whereas thermal excitation calls for a first-power dependence.

However, this does not mean that the excitation process involves three OH radicals, because in such flame gases H, O, and OH are equilibrated among themselves by way of rapid reversible bimolecular reactions, even though they are not in equilibrium with the stable products of the flame. As a result, various linear relations exist among the concentrations of H, O, and OH. Therefore, Kaskan was not able to choose any specific excitation reaction from among the various possibilities that are both energetic enough, and also account for the observed $[OH]^3$ dependence. He pointed out that further progress might be made by studying a system in which the radicals are not equilibrated with each other, providing that methods are available for the separate measurement of each radical concentration.

Schott and Kinsey[1] found that a well-defined, highly nonequilibrium region exists behind shock waves in H_2–O_2–Ar mixtures. After the gas has been compressed and heated by the shock front, there is an induction period during which the H, O, and OH concentrations increase exponentially with time because of chain branching, while the temperature, pressure, and reactant concentrations all remain virtually constant. The induction period ranges from a few to a few hundred microseconds over convenient ranges of shocked-gas properties.

As to the concentrations of free radicals, they need not be measured. Instead, they can be calculated with some confidence by integrating the small set of chemical rate equations that govern the branching process during the induction period. The required rate constants are now fairly well established.[5]

Thus, the necessary ingredients for further study of OH^* excitation in the H_2–O_2 reaction are available. This paper describes measurements of OH^* radiation intensity, and its timewise variation, in the induction zone behind shock waves traveling through 5%H_2–95% air mixture. The results are interpreted in terms of radical-recombination reactions.

EXPERIMENTAL PROCEDURE

The rectangular shock tube (approx. inside dimensions, 37×74 mm) is shown schematically in Fig. 1. It was equipped with a miniature piezoelectric pickup (T) used to trigger an oscilloscope, followed by six thin-film resistance gauges. Two of these were upstream of the test section.

[1] G. L. Schott and J. L. Kinsey, J. Chem. Phys. **29**, 1177 (1958).
[2] H. Gg. Wagner, Symp. Combust. 9th, Cornell Univ., 454 (1963).
[3] K. J. Laidler, *The Chemical Kinetics of Excited States* (Clarendon Press, Oxford, England, 1955).
[4] W. E. Kaskan, J. Chem. Phys. **31**, 944 (1959).
[5] F. Kaufman and F. P. Del Greco, Ref. 2, p. 659.

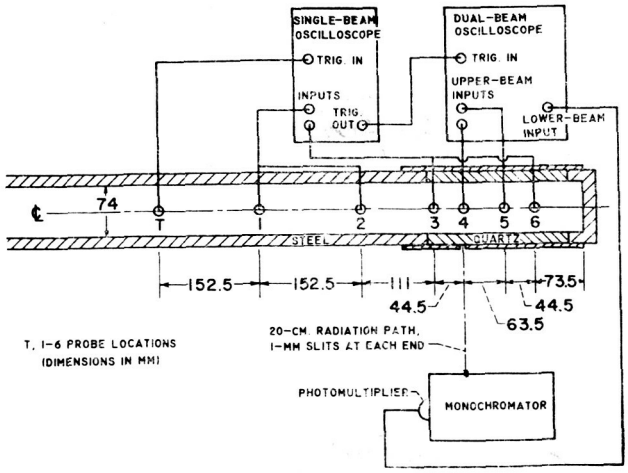

FIG. 1. Schematic drawing of end of test section of shock tube and some associated instrumentation. Top view.

Two oscilloscopes were used. On one of them, the outputs of thin-film gauges number 1, 2, 6, and, on occasion, 3, were displayed and photographed. Measurements of the time interval between shock arrival at the various stations gave either two or three velocities, over a tube length of 416 mm. The second oscilloscope had two independent electron beams and was triggered by gate signals from the first. On one beam, the outputs of gauges Nos. 4 and 5 were displayed to give a localized velocity measurement over an interval of 63.5 mm. The signal due to light emission was displayed on the other beam. Timing signals produced by a crystal-controlled secondary frequency standard were recorded on all three oscilloscope beams for each run.

The gas mixture used, 5% H_2–95% air, is quite exothermic, so there was concern that the heat release might accelerate the wave as it moved down the tube. This proved to be unfounded, so long as the initial pressure was low. All the tests reported were run at 10 Torr initial pressure; the measured velocities over the entire 416-mm instrumented length were either very nearly constant or slowly decreasing, depending on the Mach number, and showed neither acceleration nor periodic changes. Calculated temperatures in the essentially unreacted mixture just behind the shock front ranged from about 1100° to 1900°K; the corresponding pressures were about 0.2 to 0.5 atm.

Two opposite walls of the test section were made of transparent quartz plates, one of which was masked by a metal sheet containing a vertical slit 1 mm wide. This slit was located at the same axial position as thin-film gauge No. 4. Light emitted through the slit was observed by means of a grating monochromator with its entrance slit set at 1-mm width and located 20 cm away from the window. This arrangement gave very good time resolution. The monochromator viewed radiation from a wedge of gas that had an axial thickness averaging about 1.3 mm; and, since the shock speeds were 1.3 mm/μsec or greater, the time resolution was better than 1 μsec. The monochromator passed light in a 33-Å region of the 0–0 band, centered at 3080 Å. The light was detected by a Type 1P28 photomultiplier, operated in a linear part of its response curve. Figure 2 is a typical record of the dual-beam oscilloscope display obtained with relatively low gain on the photomultiplier channel. It shows, on the upper beam, the arrival of the shock at the thin-film gauge No. 4 (and at the observation slit) and the subsequent arrival at Gauge No. 5, and, on the lower beam, the photomultiplier signal.

The optical system and photomultiplier were calibrated by means of a standard incandescent lamp with known spectral radiance.[6] Like the experiments, the calibration was done without mirrors or lenses. The monochromator slit, and an additional slit between it and the lamp, were arranged so that the monochromator could not view past the edges of the filament, nor could it view the cooler regions toward the ends of the filament.

For the purposes of the present experiment, it is not necessary to have a very accurate calibration; it is sufficient to know the concentration of excited hydroxyl to within an order of magnitude. However, the assumption that the calibration is even that good must be justified in an experiment such as this, where events far from equilibrium are studied and where the total intensity of a few rotational lines is compared with the intensity of the continuum radiation from the standard lamp.

Kaskan[4] pointed out that the peak intensity of the 0–0 band measures the population of the excited state within 10% over the temperature range 1200°–1600°K, provided the rotational distribution is thermal. There is no way to determine directly whether or not the distribution was thermal in the present experiments. However, a number of preliminary tests were run to show that the emission behaved in a manner comparable to that observed by Kaskan in his flame studies.

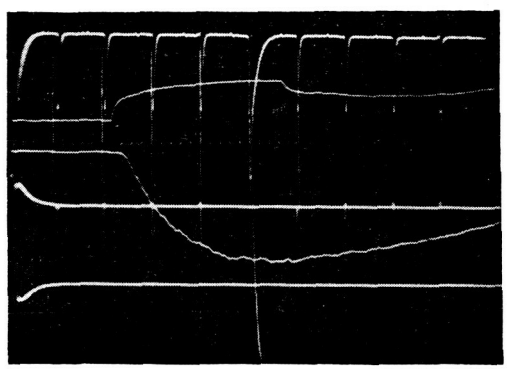

FIG. 2. Typical oscilloscope record.

[6] National Bureau of Standards lamp No. U-81.

First, a series of runs at the same shock strength, but with various settings of the monochromator slit and drum, established that the peak intensity of the 0–0 band did indeed occur in the 33-Å interval centered at 3080 Å.

Second, the peak intensities of the 0–0, 1–0, 2–1, and 3–2 bands were observed in four successive runs at the same shock strength. A semilogarithmic plot of the intensities of the latter three bands relative to that of the 0–0 band, against vibrational temperature showed that the vibrational temperature of OH* was about 3000°K in an induction zone which, in this series of runs, was at a temperature of 1200°K. Thus, OH* emitted before it had time to relax vibrationally. Kaskan[4] noted the same behavior and found similar vibrational temperatures.

Despite this vibrational disequilibrium, the rotations should become thermalized before emission. Ground-state OH relaxes in about 10 collisions,[7] and the electronically excited state should require fewer collisions than that. The lifetime of the excited state is about 5×10^{-7} second.[8] Since the collision frequency at the pressure and temperature existing behind the shock waves is about 1×10^{9}/sec, there is ample opportunity for rotation to be thermalized.

Thus, the OH* emission observed in these experiments shows no alarming symptoms, and it is concluded that the calibration is sufficiently good for the purposes of this work. It was found that the photomultiplier produced a signal of 1 mV in response to a source in the shock tube emitting 8.5×10^{10} photons/cm^3·sec into the whole solid angle in the whole 33-Å band centered at 3080 Å. Assuming a constant transition probability[8] of 1.8×10^{6} sec^{-1} for all lines in the band, this corresponds to $[OH^*]=7.8\times10^{-17}$ mole/liter. No allowance was made for self-absorption, which was expected to be small, at least during the early part of the induction period when the OH concentration is low. If it were present and taken into account, however, this self-absorption would increase the [OH*] corresponding to a given photomultiplier signal, and hence would reinforce the conclusions drawn from this work.

RESULTS

Data on intensity of emitted light vs time were read from oscillograms such as Fig. 2. Zero time is the instant that an element of gas passes through the shock front, and this was fixed by the time of shock arrival at the thin-film Gauge No. 4. Times measured from the oscillograms were multiplied by the density ratio across the shock to convert them to true gas times. The density, pressure, and temperature ratios were calculated from the measured Mach number by the graphical method of Markstein.[9] In making these calculations, it was assumed that no significant chemical reaction occurred during the induction period and that the gas reached full thermal equilibrium. The range of shock-wave Mach numbers was about 3.8 to 5.5, corresponding to induction-zone temperatures from about 1100° to 1900°K.

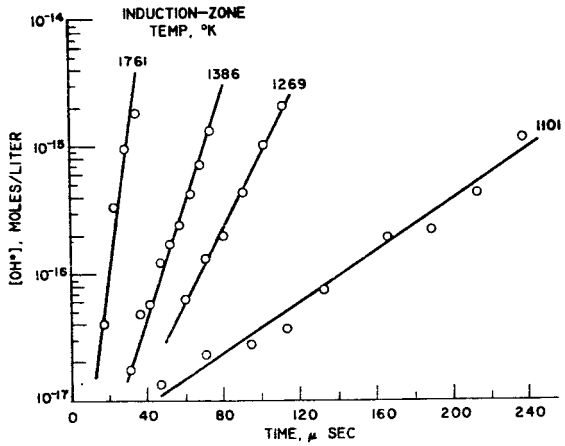

FIG. 3. Growth of excited hydroxyl-radical concentration during induction period.

Typical [OH*]-time data are shown in Fig. 3 for several temperatures. Oscilloscope voltages have been reduced to concentrations of excited hydroxl radical, [OH*], by means of the calibration factor. It was found that [OH*] grows exponentially with time over an increase of about two observable orders of magnitude in [OH*], after which an inflection occurs and then a maximum is reached. It is the early exponential part of the history that is of first interest in the present work. During this period, $[OH^*]\propto \exp(t/\tau)$. The exponential time constants, $1/\tau$ sec^{-1}, were obtained from the slopes of lines such as those shown in Fig. 3, drawn through the data by inspection.

DISCUSSION

Chain-Branching Process

During the induction period of the H_2–O_2 reaction, the concentrations of the free radicals H, O, and OH grow rapidly by chain branching. The rate of this process is governed by the rates of a few rapid bimolecular reactions. Before these reactions can become effective, however, a small concentration of free radicals must be built up by some initiation process in which molecular species react. At sufficiently high temperatures, the dissociation of hydrogen is no doubt an important means of initiation; but, for the range up to 1900°K covered in the present work, it was assumed that only the following reaction contributes:

$$H_2+O_2\rightarrow 2OH. \qquad (I)$$

[7] G. B. Kistiakowsky and F. D. Tabbutt, J. Chem. Phys. **30**, 577 (1959).

[8] T. Carrington, J. Chem. Phys. **31**, 1243 (1959).

[9] G. H. Markstein, ARS J. **29**, 588 (1959).

TABLE I. Rate constants, $k_i = A_i \exp(-E_i/RT)$ (liters/mole·sec).

Reaction	$\log_{10} A_i$	E_i (kcal/mole)	Ref.
(I)	11.0	70.0	12
(II)	11.3	16.6	13
(III)	9.4±0.7	7.7±1.0	5
(IV)	10.8±0.7	5.9±1.0	5
(V)	9.9±0.3	1.0±0.5	5

Schott and Kinsey[1] identified the end of the induction period with the attainment of $[OH]=10^{-6}$ mole/liter. The recent interferometric data of White[10] on low-pressure H_2–O_2 detonations confirm that there is no appreciable heat release for times comparable to Schott and Kinsey's induction times. Accepting their definition of the induction period, then, it turns out that initiation occupies only a small part of the period. The growth of free-radical concentrations during most of the period is strictly exponential, with a time constant that is greatly influenced by the rate of the slow chain-branching reaction

$$H+O_2 \rightarrow OH+O. \qquad \text{(II)}$$

However, if $([H_2]/[O_2]) < 1$, as in these experiments, the following reactions also affect the process:

$$O+H_2 \rightarrow OH+H, \qquad \text{(III)}$$

$$OH+H_2 \rightarrow H_2O+H. \qquad \text{(IV)}$$

Finally, the following reaction may be included for the sake of completeness:

$$OH+OH \rightarrow H_2O+O. \qquad \text{(V)}$$

It turns out to be without effect on the results, because even though its rate constant is large, its rate is very small owing to the small values of [OH] that exist during the induction period.

Reactions (I) to (V) were used to set up the differential equations describing the growth of [H], [O], and [OH] during the induction period. These were integrated numerically by means of an IBM 7090 program, using the Runge–Kutta method.[11] The rate constants used[5,12,13] are listed in Table I.

Figure 4 is a semilogarithmic plot of the calculated quantities for an induction-zone temperature of 1500°K and is typical of the results for other temperatures. It is seen that the plots are linear except for a brief initiation period and that all three lines have the same slope.

[10] D. R. White, Rept. No. 63-RL-3288C, General Electric Research Laboratory, April 1963.

[11] J. B. Scarborough, *Numerical Mathematical Analysis* (The John Hopkins University Press, Baltimore, Maryland 1930).

[12] R. E. Duff, J. Chem. Phys. **28**, 1193 (1958).

[13] R. R. Baldwin, Ref. 2, p. 687.

Therefore,

$$\frac{[OH]}{[OH]_0} = \frac{[O]}{[O]_0} = \frac{[H]}{[H]_0} = e^{t/\tau}, \qquad (1)$$

where the concentrations with subscript zero are the values obtained by extrapolation to zero time. The fact that a single time constant τ suffices to describe the growth of all three free-radical concentrations greatly simplifies the prediction of OH* concentration. Table II lists the pseudoinitial concentrations and the time constants obtained from calculations using two different sets of rate constants from Table I.

Production of OH* by Radical Recombination

In order to excite ground-state OH to the $^2\Sigma^+(v=0)$ state, 88.3 kcal/mole are required. Therefore, the chemiluminescent production of OH* can only be accomplished by a few energetic reactions that involve either the transfer of heat of recombination to OH acting as a third body or the direct production of OH* in a highly exothermic reaction. The possibilities in the first category are

$$H+H+OH \rightarrow H_2+OH^*, \qquad \text{(VIa)}$$

$$O+O+OH \rightarrow O_2+OH^*, \qquad \text{(VIb)}$$

$$H+OH+OH \rightarrow H_2O+OH^*, \qquad \text{(VIc)}$$

and

$$O+H_2+OH \rightarrow H_2O+OH^*. \qquad \text{(VIIa)}$$

In the second category are

$$O+H+M \rightarrow OH^*+M, \qquad \text{(VIIb)}$$

and

$$H+O_2+H_2 \rightarrow H_2O+OH^*. \qquad \text{(VIII)}$$

The rates of Reactions (VI) involve three free-radical concentration terms; the rates of Reactions (VII) involve two; and the rate of Reaction (VIII), only one.

In calculating the rate of growth of [OH*], it is reasonable to include a quenching reaction. It has been

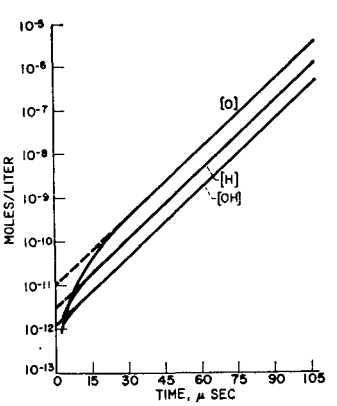

FIG. 4. Calculated concentrations of ground-state free radicals during induction period in 5% H_2–95% air. Temperature, 1500°K; initial pressure, 10 Torr.

TABLE II. Calculated parameters describing free-radical concentrations during induction period. Initial pressure, 10 Torr.

Shocked gas Temperature (°K)	Pressure (atm)	$[H]_0$ (moles/liter) (a)	(b)	$[O]_0$ (moles/liter) (a)	(b)	$[OH]_0$ (moles/liter) (a)	(b)	$1/\tau$ (sec^{-1}) (a)	(b)
1100	0.2307	3.16×10^{-15}	2.12×10^{-15}	4.58×10^{-15}	1.55×10^{-15}	3.98×10^{-16}	2.82×10^{-16}	2.5×10^{4}	3.9×10^{4}
1300	0.2930	1.82×10^{-13}	1.02×10^{-13}	3.63×10^{-13}	1.19×10^{-12}	3.89×10^{-14}	2.74×10^{-14}	6.3×10^{4}	10.4×10^{4}
1500	0.3556	3.16×10^{-12}	1.89×10^{-12}	1.00×10^{-11}	2.72×10^{-12}	1.24×10^{-12}	7.93×10^{-13}	12.2×10^{4}	20.4×10^{4}
1700	0.4193	3.04×10^{-11}	1.59×10^{-11}	1.06×10^{-10}	3.16×10^{-11}	1.75×10^{-11}	1.00×10^{-11}	18.9×10^{4}	33.9×10^{4}
1900	0.4873	1.86×10^{-10}	9.50×10^{-11}	7.73×10^{-8}	2.00×10^{-10}	1.34×10^{-10}	7.48×10^{-11}	27.4×10^{4}	49.8×10^{4}

[a] Best values for k's, Table I.
[b] k_1, k_2, k_4, k_5 best values; $\log_{10}A_3=10.1$, $E_3=8.7$.

found[14,15] that OH* is very effectively quenched by H_2O. For the present, however, it is assumed that quenching occurs by the following nonspecific reaction:

$$OH^*+M\rightarrow OH+M. \qquad (IX)$$

In view of the results of the calculations of free-radical concentrations, as expressed by Eq. (1), the growth of [OH*] is given as follows if the excitation reaction is (VIa), (VIb), or (VIc):

$$d[OH^*]/dt=k_eC_3e^{3t/\tau}-k_9[OH^*][M]. \qquad (2)$$

Here, k_e is the rate constant of the excitation reaction and k_9 that of the quenching reaction. The term C consists of the product of three concentration terms; for example, $C_3=[H]_0^2[OH]_0$ if the excitation reaction is (VIa). The subscript 3 denotes the fact that all three terms refer to free-radical concentrations.

Similarly, Reactions (VIIa) and (VIIb) lead to

$$d[OH^*]/dt=k_eC_2e^{2t/\tau}-k_9[OH^*][M], \qquad (3)$$

and Reaction (VIII) leads to

$$d[OH^*]/dt=k_eC_1e^{t/\tau}-k_9[OH^*][M]. \qquad (4)$$

Integration[16] of Eq. (2), (3), or (4) between the limits of 0 and t yields

$$[OH^*]=\frac{k_eC_n\{\exp(nt/\tau)-\exp(-k_9[M]t)\}}{n/\tau+k_9[M]}, \qquad (5)$$

in which n may be 1, 2, or 3, depending upon the type of excitation reaction assumed.

Comparison of Observed and Predicted [OH*]

There are two ways in which the experimental data may be compared with the predictions of Eq. (5). First, the observed OH* concentrations may be compared in magnitude with the calculated values. Second, the rates of growth may be compared.

Comparison of Magnitudes

It can be appreciated that the calculated value of [OH*] at a given time during the induction period may vary by several orders of magnitude, depending upon the type of excitation reaction assumed. For instance, Fig. 4 shows that, at 1500°K, $[H]_0\approx10^{-12}$, $[O]_0\approx10^{-11}$, and $[OH]_0\approx10^{-12}$ mole/liter. Consequently, if it is assumed that excitation occurs via one of the three-free-radical reactions, (VI), then C_3 will be of the order of 10^{-35} at this temperature. On the other hand, if Reaction (VIIa) or (VIIb) is assumed, C_2 will be of the order of 10^{-27} to 10^{-26} ($[M]\approx10^{-3}$, $[H_2]\approx10^{-4}$ mole/liter). Although $\exp(3t/\tau)$ is considerably larger than $\exp(2t/\tau)$, it is not enough greater to counteract this difference between C_3 and C_2 during the induction period.

It is instructive to calculate upper limits for [OH*], assuming each of the possible excitation reactions in turn, and to compare the results with observed concentrations. This can be done by assuming that there is no quenching—i.e., $k_9=0$—and that $k_e=1\times10^{10}$ liter^2/mole^2·sec, corresponding to a very effective three-body reaction at 1500°K. Equation (5) then becomes

$$[OH^*]=\frac{1\times10^{10}C_n[\exp(nt/\tau)-1]}{n/\tau}. \qquad (6)$$

Figure 5 shows curves calculated from Eq. (6), using data from Table II(a). Also shown is a line drawn through experimental data obtained at 1497°K.

It is seen that the observed OH* concentrations lie many orders of magnitude above the values expected for the three-free-radical reactions, (VIa), (VIb), and (VIc). They also lie well above the curves computed for the two-free-radical processes, (VIIa) and (VIIb). Moreover, it should be noted that, if OH* were

[14] H. P. Broida and T. Carrington, J. Chem. Phys. **23**, 2202 (1955).
[15] T. Carrington, J. Chem. Phys. **30**, 1087 (1959).
[16] G. M. Murphy, *Ordinary Differential Equations and Their Solutions* (D. Van Nostrand, Inc., Princeton, New Jersey, 1960), p. 226.

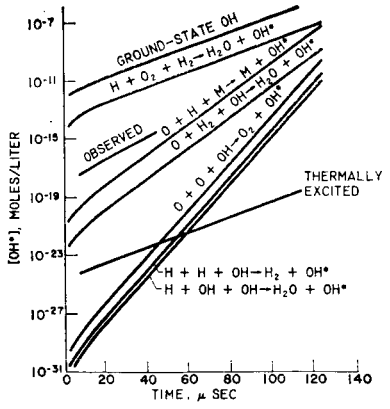

FIG. 5. Calculated and observed [OH*] during induction period in 5% H_2–95% air. Temperature, 1500°K; initial pressure, 10 Torr.

formed thermally, its concentration would be about $\exp(-88\,000/RT)$ times the ground-state OH concentration, or about 13 orders of magnitude below the uppermost curve of Fig. 5. Data for other temperatures behave in the same manner. Consequently, comparison of observed [OH*] with the maximum values that can reasonably be calculated favors Reaction (VIII) as the one responsible for excitation.

Discussion of the fact that the observed [OH*] are less than the upper-limit values predicted on the basis of Reaction (VIII) will be deferred to the section on quenching.

Comparison of Rates of Growth

If excitation does in fact occur by way of Reaction (VIII), n should be unity in Eq. (6). Observed [OH*] and calculated concentrations of ground-state free radicals, plotted semilogarithmically against time, should have the same slope at a given temperature. The extent to which this is borne out is shown in Fig. 6. The observed time constants are well bracketed by two lines—one calculated using the average values of the rate constants in Table I, the other calculated using the upper-limit value for k_3, $1.25\times10^{10}\exp(-8700/RT)$. It can be seen from Fig. 6 that a somewhat smaller change in k_3 would have fit the data better, but no effort was made to optimize the fit.

The uppermost curve of Fig. 6 shows the exponential time constants that result if only Reaction (II) is important. Schott and Kinsey[1] pointed out that it would be rate-controlling if $([H_2]/[O_2])\geq1$, and that $1/\tau$ would then be equal to $2k_2[O_2]$. Obviously, the fact that $([H_2]/[O_2])<1$ in the present experiments has a very great effect on the chain-branching process.

Quenching of OH*

The discrepancy in Fig. 5 between the observed [OH*] and the values predicted on the basis of Reaction (VIII) can be explained by generalized quenching [Reaction (IX)]. If it is assumed that k_9 corresponds to the collision number, say, 5×10^{11} liter/mole·sec, then the term $k_9[M]$ in the denominator of Eq. (5) will be much larger than $1/\tau$. Moreover, the term $\exp(-k_9[M]t)$ will be negligible compared to $\exp(t/\tau)$ at all times greater than 1 μsec. Equation (5) then becomes

$$[OH^*]=k_8[H]_0[O_2][H_2]e^{t/\tau}/5\times10^{11}[M] \qquad (7)$$

when written in the form appropriate for Reaction (VIII). Solving Eq. (7) for k_8 and inserting experimental data from Fig. 5 and the value of $[H]_0$ from Table II(b) yield $k_8\approx0.8\times10^{10}$ liter²/mole²·sec at 1500°K, corresponding to a very efficient three-body reaction. It is interesting to note that Kaskan[4] reached exactly the same conclusion when he used his light-intensity measurements to deduce k_e, after setting the rate constant for the quenching reaction equal to the binary collision number.

If the picture of the excitation and quenching of OH* that is embodied in Eq. (7) is correct, then neither k_8 nor k_9 should depend much on the temperature. Values of k_8 calculated from Eq. (7) by using experimental data should be nearly constant over the whole range of temperatures from 1100° to 1900°K. But in actual fact these "experimental" k_8's, although they scatter badly, indicate a strong trend with temperature. In order to explain the data, they must be rather greater than 10^{10} liter²/mole²·sec at 1100°K, and two or three orders of magnitude less at the upper end of the temperature range.

If, on the other hand, it is assumed that there is no quenching ($k_9=0$), the k_8's naturally turn out to be much smaller, but they still have the same strong temperature dependence.

To put the situation another way: The intensity of OH* emission is unexpectedly small at high temperatures and unexpectedly large at low temperatures. One ready explanation for these facts is that quenching occurs by collisions with a reaction product. The obvious

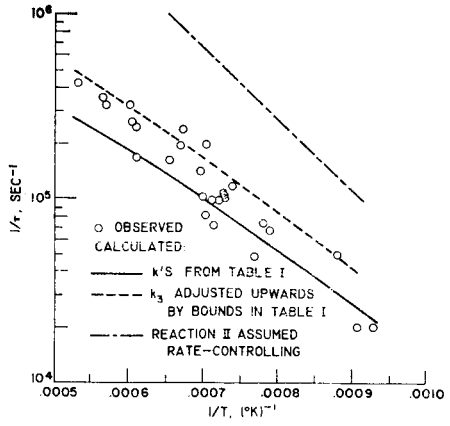

FIG. 6. Comparison of observed and predicted rates of growth of [OH*].

candidate is of course H_2O, which is known to be a very effective quencher from flame studies.[14,15]

Another reason for suspecting that the observed behavior is due to quenching by H_2O is that the light-intensity–time traces go through an inflection point quite early, well before the end of the induction period at $[OH]=10^{-6}$ mole/liter. In the present experiments at, say, 1500°K, the calculations of Table II(b) show that this concentration is reached after about 70 μsec. But near 1500°K, the light-intensity curves go through an inflection at around 45 μsec. If this change in the rate of increase of [OH*] were merely due to the disappearance of free radicals in the heat-releasing recombination part of the reaction, it should occur closer to 70 μsec. The same thing is found at all temperatures, except perhaps the very highest ones: namely, the inflection point occurs well before the end of the induction period. This, too, can be qualitatively explained by supposing that the H_2O concentration, which also rises exponentially during the induction period, finally becomes great enough to exert an observable quenching effect.

In order to test this idea quantitatively, it is necessary to derive a new expression for the prediction of [OH*], assuming that Reaction (IX) is replaced by the following quenching reaction:

$$OH^*+H_2O\rightarrow OH+H_2O. \qquad (X)$$

Since H_2O is produced almost solely by Reaction (IV) during the induction period,

$$d[H_2O]/dt=k_4[OH][H_2]=k_4[OH]_0[H_2]e^{t/\tau}. \qquad (8)$$

Integrating between limits of 0 and t,

$$[H_2O]=k_4[OH]_0[H_2]\tau(e^{t/\tau}-1). \qquad (9)$$

Therefore,

$$d[OH^*]/dt=k_8[H]_0[O_2][H_2]e^{t/\tau}$$
$$-k_{10}k_4[OH]_0[H_2][OH^*]\tau(e^{t/\tau}-1). \qquad (10)$$

Equation (10) cannot be readily integrated. However, useful results can be obtained from the form of Eq. (10) that is applicable to times great enough so $e^{t/\tau}\gg 1$. If, for example, this inequality is taken to be satisfied when $e^{t/\tau}=5$, then, using values of $1/\tau$ from Table II(b), the inequality holds from 41.3 μsec on at 1100°K, and from 3.2 μsec on at 1900°K. It will be assumed that the form of Eq. (10) obtained by dropping the factor of unity in the second term on the right-hand side applies to the region in which the inflection point occurs. Differentiating and setting the result equal to zero, one obtains

$$t_{infl}=\frac{2.303}{1/\tau}\log_{10}\left\{\frac{(1/\tau)^2}{k_{10}k_4[OH]_0[H_2]}\right\} \qquad (11)$$

and

$$k_8=\frac{k_{10}k_4[OH]_0[OH^*]_{infl}}{1/\tau[H]_0[O_2]}. \qquad (12)$$

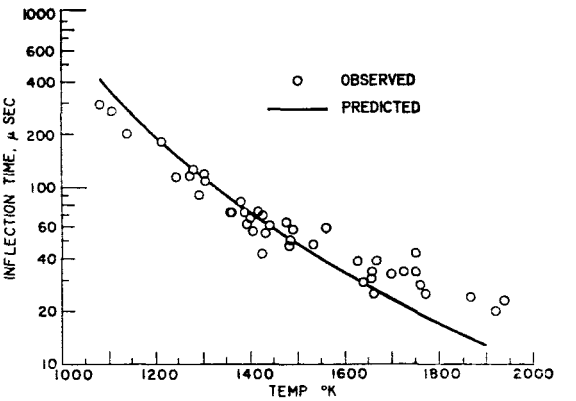

FIG. 7. Comparison of observed and predicted time of inflection point in OH* concentration.

It is seen that Eq. (11) permits the time at which the inflection point occurs to be calculated without recourse to any experimental data. This has been done, using the data from Table II(b) and assuming k_{10} is the collision number. The results are plotted in Fig. 7. Experimental inflection times were estimated directly from the photomultiplier records and multiplied by the density ratio across the shock to convert from laboratory to gas time. The data points plotted in Fig. 7 include those from the runs used to obtain [OH*]–time data, and also those from a large number of runs made to measure induction times; in the latter, the oscilloscope gain was too small to give detailed intensity–time data in the early part of the induction period, but the inflection point could be read. All in all, the observed times agree well with those predicted by means of Eq. (11). Although the points tend to drift away from the curve at the higher temperatures, this may be partly due to the fact that the approximation used ($e^{t/\tau}\gg 1$) becomes worse at these temperatures.

Finally, Eq. (12) was used to estimate values for k_8. Once again, the data from Table II(b) were used, and k_{10} was taken as the binary collision number. The concentration of OH* at the inflection point could be read to within a factor of about 2 at the higher temperatures, more closely at the lower ones. In contrast to the calculations of k_8 made with the previously discussed assumptions about the quenching, the calculations made with Eq. (12) produced much more nearly constant values. The range of k_8 was 4×10^4 to 9×10^5, with no discernible temperature dependence. The average for 23 runs in which [OH*] could be read at the inflection point was 2×10^5 liter^2/mole^2·sec.

Thus, the data make sense when viewed with the idea that OH* is effectively quenched only upon collision with H_2O. This treatment leads to a rate constant for the excitation reaction that corresponds to an inefficient process, with a steric factor of about 10^{-5}. Since the excitation reaction (VIII) involves extensive rearrangement of bonds, it is very reasonable that it should be an inefficient process.

CONCLUSIONS

The formation of electronically excited hydroxyl radical during the induction period behind shock waves in 5% H_2–95% air mixture occurs via the three-body reaction

$$H+O_2+H_2 \rightarrow H_2O+OH^*.$$

It seems likely that the same mechanism will also hold for mixtures containing other $[H_2]/[O_2]$ ratios, because for any practical case the concentrations of hydrogen and oxygen in the induction zone will always greatly exceed the concentrations of any of the free radicals. Therefore, the rates of the other possible excitation reactions will generally be too small to contribute to the emission, even if they are efficient three-body reactions.

The rate of increase in OH^* concentration during the early part of the induction period can be successfully predicted by using literature values for the rate constants of the chain-branching reactions.

The data indicate that OH^* is effectively quenched only by H_2O in these experiments and that the excitation reaction is an inefficient one, with a rate constant averaging 2×10^5 liter^2/mole^2·sec over the temperature range from about 1100° to 1900°K.